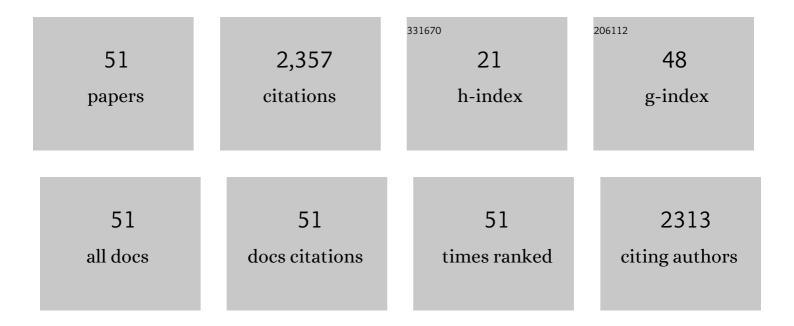
Quan-Liang Zhao

List of Publications by Year in descending order

Source: https://exaly.com/author-pdf/1098464/publications.pdf Version: 2024-02-01



#	Article	IF	CITATIONS
1	Bismuth ferrite-based lead-free ceramics and multilayers with high recoverable energy density. Journal of Materials Chemistry A, 2018, 6, 4133-4144.	10.3	325
2	High Energy Storage Density and Large Strain in Bi(Zn _{2/3} Nb _{1/3})O ₃ -Doped BiFeO ₃ –BaTiO ₃ Ceramics. ACS Applied Energy Materials, 2018, 1, 4403-4412.	5.1	229
3	Magnetic and conductive graphene papers toward thin layers of effective electromagnetic shielding. Journal of Materials Chemistry A, 2015, 3, 2097-2107.	10.3	208
4	Atomic Layer Tailoring Titanium Carbide MXene To Tune Transport and Polarization for Utilization of Electromagnetic Energy beyond Solar and Chemical Energy. ACS Applied Materials & Interfaces, 2019, 11, 12535-12543.	8.0	187
5	Temperature dependent, large electromechanical strain in Nd-doped BiFeO3-BaTiO3 lead-free ceramics. Journal of the European Ceramic Society, 2017, 37, 1857-1860.	5.7	167
6	BiFeO ₃ -BaTiO ₃ : A new generation of lead-free electroceramics. Journal of Advanced Dielectrics, 2018, 08, 1830004.	2.4	166
7	Nonlinear resonant and high dielectric loss behavior of CdSâ^α-Fe2O3 heterostructure nanocomposites. Applied Physics Letters, 2008, 93, 183118.	3.3	137
8	Sol–gel synthesis of Nd-doped BiFeO3 multiferroic and its characterization. Ceramics International, 2015, 41, 8768-8772.	4.8	112
9	Composition and temperature dependence of structure and piezoelectricity in (1â^'x)(K _{1â^'y} Na _y)NbO ₃ â€x(Bi _{1/2} Na _{1/2})ZrO <s leadâ€free ceramics. Journal of the American Ceramic Society, 2017, 100, 627-637.</s 	ub s.8 <td>0>93</td>	0>93
10	Effect of ZnO whisker content on sinterability and fracture behaviour of PZT peizoelectric composites. Journal of Alloys and Compounds, 2010, 504, 123-128.	5.5	56
11	Tuning broadband microwave absorption via highly conductive Fe3O4/graphene heterostructural nanofillers. Materials Research Bulletin, 2015, 72, 316-323.	5.2	55
12	Mechanical reinforcement and piezoelectric properties of nanocomposites embedded with ZnO nanowhiskers. Scripta Materialia, 2008, 59, 780-783.	5.2	54
13	Flexible Semitransparent Energy Harvester with High Pressure Sensitivity and Power Density Based on Laterally Aligned PZT Single-Crystal Nanowires. ACS Applied Materials & Interfaces, 2017, 9, 24696-24703.	8.0	48
14	Enhanced Piezoelectric and Ferroelectric Properties of Nb ₂ O ₅ Modified Lead Zirconate Titanateâ€Based Composites. Journal of the American Ceramic Society, 2011, 94, 647-650.	3.8	43
15	Fast-moving piezoelectric micro-robotic fish with double caudal fins. Robotics and Autonomous Systems, 2021, 140, 103733.	5.1	42
16	Construction of three-dimensional graphene interfaces into carbon fiber textiles for increasing deposition of nickel nanoparticles: flexible hierarchical magnetic textile composites for strong electromagnetic shielding. Nanotechnology, 2017, 28, 045710.	2.6	34
17	Enhanced piezoelectric and mechanical properties of ZnO whiskers and Sb2O3 co-modified lead zirconate titanate composites. Materials Letters, 2010, 64, 1798-1801.	2.6	31
18	Highly sensitive humidity sensor based on graphene oxide foam. Applied Physics Letters, 2017, 111, .	3.3	28

QUAN-LIANG ZHAO

#	Article	IF	CITATIONS
19	Effects of thickness on energy storage of (Pb, La)(Zr, Sn, Ti)O 3 antiferroelectric films deposited on LaNiO 3 electrodes. Ceramics International, 2016, 42, 1314-1317.	4.8	26
20	Dielectric and piezoelectric properties of manganeseâ€modified PbHfO ₃ –PbTiO ₃ –Pb(Mg _{1/3} Nb _{2/3})O ₃ ternary ceramics with morphotropic phase boundary compositions. Physica Status Solidi - Rapid Research Letters, 2013, 7, 221-223.	2.4	22
21	Thermodynamic analysis of the emptying process of compressed hydrogen tanks. International Journal of Hydrogen Energy, 2019, 44, 3993-4005.	7.1	21
22	Review on studies of the emptying process of compressed hydrogen tanks. International Journal of Hydrogen Energy, 2021, 46, 22554-22573.	7.1	21
23	Effect of sintering temperature and time on densification, microstructure and properties of the PZT/ZnO nanowhisker piezoelectric composites. Journal of Alloys and Compounds, 2011, 509, 6980-6986.	5.5	19
24	Broadening Electromagnetic Absorption Bandwidth: Design from Microscopic Dielectricâ€Magnetic Coupled Absorbers to Macroscopic Patterns. Physica Status Solidi (A) Applications and Materials Science, 2017, 214, 1700589.	1.8	16
25	Coordinated variable impedance control for multi-segment cable-driven continuum manipulators. Mechanism and Machine Theory, 2020, 153, 103969.	4.5	16
26	Fabrication, Microstructure and Properties of Zinc Oxide Nanowhisker Reinforced Lead Zirconate Titanate Nanocomposites. Current Nanoscience, 2011, 7, 227-234.	1.2	14
27	Assembling carbon fiber–graphene–carbon fiber hetero-structures into 1D–2D–1D junction fillers and patterned structures for improved microwave absorption. Journal Physics D: Applied Physics, 2017, 50, 135303.	2.8	14
28	A highly conductive self-assembled multilayer graphene nanosheet film for electronic tattoos in the applications of human electrophysiology and strain sensing. Nanoscale, 2021, 13, 10798-10806.	5.6	14
29	Effects of Nb2O5 addition on the microstructure, electrical, and mechanical properties of PZT/ZnO nanowhisker piezoelectric composites. Journal of Materials Science, 2012, 47, 2687-2694.	3.7	13
30	Fabrication and characterization of a piezoelectric micromirror using for optical data tracking of high-density storage. Microsystem Technologies, 2014, 20, 1317-1322.	2.0	12
31	Ultrafastâ€Response Humidity Sensor with High Humidity Durability Based on a Freestanding Film of Graphene Oxide Supramolecular. Physica Status Solidi (A) Applications and Materials Science, 2020, 217, 1900869.	1.8	12
32	Variable Impedance Control of Cable Actuated Continuum Manipulators. International Journal of Control, Automation and Systems, 2020, 18, 1839-1852.	2.7	12
33	Dielectric, piezoelectric, and ferroelectric properties of Al ₂ O ₃ and MnO ₂ modified PbSnO ₃ -PbTiO ₃ -Pb(Mg _{1/3}) Tj ETQq1 1 0	.784314 rg	gBT/Overlock
	Materials Science. 2013. 210. 1363-1368.		
34	Effects of electrodes on ferroelectric properties of PNZT films prepared by sol–gel method. Journal of Sol-Gel Science and Technology, 2016, 78, 258-261.	2.4	11
35	Dynamics Analysis and Control of a Bird Scale Underactuated Flapping-Wing Vehicle. IEEE Transactions on Control Systems Technology, 2020, 28, 1233-1242.	5.2	11
36	Piezoelectric, ferroelectric and mechanical properties of lead zirconate titanate/zinc oxide nanowhisker ceramics. Journal of Materials Science: Materials in Electronics, 2011, 22, 1393-1399.	2.2	10

QUAN-LIANG ZHAO

#	Article	IF	CITATIONS
37	Electrical Properties of Lead Zirconate Titanate Thick Film Containing Micro- and Nano-Crystalline Particles. Chinese Physics Letters, 2012, 29, 058101.	3.3	10
38	Thickness-dependent electrical properties of sol–gel derived Pb(Zr0.52Ti0.48)O3 thick films using PbTiO3 buffer layers. Journal of Materials Science: Materials in Electronics, 2013, 24, 3521-3525.	2.2	9
39	Robust Trajectory Tracking of Delta Parallel Robot Using Sliding Mode Control. , 2019, , .		8
40	Highly efficient and giant negative electrocaloric effect of a Nb and Sn co-doped lead zirconate titanate antiferroelectric film near room temperature. RSC Advances, 2019, 9, 34114-34119.	3.6	7
41	Hydrodynamics Modeling of a Piezoelectric Micro-Robotic Fish With Double Caudal Fins. Journal of Mechanisms and Robotics, 2022, 14, .	2.2	7
42	A highly directional metamaterial-based terahertz circulator that does not require an external magnetic field. Journal Physics D: Applied Physics, 2021, 54, 105103.	2.8	6
43	Energy storage and thermodynamics of PNZST thick films with coexisting antiferroelectric and ferroelectric phases. International Journal of Applied Ceramic Technology, 2021, 18, 154-161.	2.1	5
44	Finite-Time Observer-Based Variable Impedance Control of Cable-Driven Continuum Manipulators. IEEE Transactions on Human-Machine Systems, 2022, 52, 26-40.	3.5	5
45	Drive-mode control for an underactuated MEMS vibratory rate gyroscope. Microsystem Technologies, 2016, 22, 1151-1161.	2.0	2
46	Dynamics and Switching Control of a Class of Underactuated Mechanical Systems with Variant Constraints. Applied Sciences (Switzerland), 2019, 9, 4235.	2.5	2
47	Thermodynamic Analysis of Stressâ€Mediated Barocaloric Effect, Electrocaloric Effect, and Energy Storage of PbZrO ₃ Antiferroelectric Film. Physica Status Solidi (A) Applications and Materials Science, 2021, 218, 2000651.	1.8	2
48	Synthesis and electrical properties of Pb(Zr0.52Ti0.48)O3 thick films embedded with ZnO nanoneedles prepared by the hybrid sol–gel method. Journal of Materials Science: Materials in Electronics, 2013, 24, 2521-2526.	2.2	1
49	Research on the optimization method of top-drive variable-capacitance micromotors. Microsystem Technologies, 2015, 21, 2443-2453.	2.0	1
50	Manipulating microstructures and electrical properties of carbon fiber/reduced graphene oxide/nickel composite textiles with electrochemical deposition techniques. Applied Physics A: Materials Science and Processing, 2017, 123, 1.	2.3	1
51	An Adaptive Time-Varying Impedance Controller for Manipulators. Frontiers in Neurorobotics, 2022, 16, 789842.	2.8	1